Microstructural analyses and wear behavior of the cemented carbide tools after laser surface treatment and PVD coating

Davi Neves [a,b], Anselmo Eduardo Diniz [a,*], Milton Sérgio Fernandes Lima [b]

[a] Faculty of Mechanical Engineering, University of Campinas, P.O. Box 6122, 13083-970 Campinas, SP, Brazil
[b] Institute for Advanced Studies (IEAv/DCTA), P.O. Box 6044, 12229-970 Sao Jose dos Campos, SP, Brazil

ARTICLE INFO

ABSTRACT

Adhesion is one of the most important characteristics of coating on cutting tools. Poor coating adhesion on the tool favors fragmentation and release of hard abrasive particles between the tool and the work-piece. These particles interact with the surfaces of the tool, accelerating its wear and decreasing tool life. One possible solution is the use of laser texturing prior to coating in order to achieve a desired surface topography with enhanced adhesion properties. In the texturing, a high-frequency short-pulse laser changes surface characteristics, generating resolidified material and selective vaporization. This work evaluated the effectiveness of laser texturing in improving the substrate–coating adhesion of PVD coated cemented carbide tools. To this end, the substrates were textured with a Nd:YAG laser, in four different intensities, and then coated with a PVD TiAlN film. To ascertain the effectiveness of laser texturing, Rockwell C indentation and turning experiments were performed on both textured tools and conventional unlasered tools. The PVD coated laser-textured tool showed better performance in the indentation and turning tests than the standard tools. A comparative evaluation of tool wear mechanisms indicated that texturing did not change the wear mechanisms, but altered their importance to tool wear. The anchoring provided by the higher roughness of the textured surface increased the adhesion of the coating on the substrate, thus increasing tool life. Additionally, the chemical modification of the carbide grains due to the laser heating might be responsible for an enhanced adhesion between coating and substrate.

© 2013 Elsevier B.V. All rights reserved.

1. Introduction

The treatment of surfaces is one of the main factors for controlling the adhesion between coating and substrate on a cutting tool. The tool's surface properties can be modified by different types of surface treatment, thereby improving the adhesion and, consequently, the tool's performance [1]. Several processes have been employed to treat the substrate before applying the coating and to increase the interfacial bond toughness like water peening in cermets [2], water peening and chemical etching for diamond coating [3], grinding, micro-blasting and water peening for (Ti,Al)N coating [4], micro-blasting at low and high pressure, polishing, as well as combinations of micro-blasting with glass-blasting at low pressure [5] cathodic arc ion etching and magnetron sputtering [6,7]. One of the most usual processes is abrasive sandblasting. The effect of this process on the target surface depends on the size and kinetic energy of the abrasive grain. High energy impacts of a large grain on the cemented carbide surface cause large plastic deformation and induce compressive residual stresses. The use of small abrasive

grains reduces plastic deformation of the surface and the presence of abrasive fragments on it [4]. When this process is applied to cemented carbide substrates, some Co is removed from the surface because it is softer than the other phases, such as WC, TiC and TaC. This process contributes to eliminate high carbides peaks by erosion and to create new valleys where Co particles were ablated, contributing to the adhesion between substrate and coating. The enhanced adhesion is then due to better mechanical anchoring of the coating to the substrate enabled by an optimized topography [5].

The use of water jet or abrasive blasting, although very known in toolmakers industries, remains on the manual ability of operators and usually produces poorly reproducible surface patterns. Additionally surface contaminations could be a serious issue to the tool performance. Finally, green manufacturing guidelines usually point out reduction of water and consumables as goals for sustainable industrial procedures.

The use of laser to prepare the substrate surface to receive the coating has proved to be an advantageous alternative for surface preparation [8]. Laser ablation is not only suitable for process automation, treatment of selected areas and complex surface processing, but also enables the precise removal of material with practically no thermal damage of adjacent zones [9]. When

* Corresponding author. Tel.: +55 19 35213303; fax: +55 19 32893722.
E-mail address: anselmo@fem.unicamp.br (A.E. Diniz).

materials are laser processed, different laser–material interaction mechanisms, thermal or non-thermal, can be triggered by varying the process parameters (beam power, intensity distribution, pulse form, frequency and duration), which determine the physical nature of the process [10].

The laser treatment of WC–Co surfaces is a non-contact technique which transfers large amounts of energy to a small region delimited by the laser beam diameter. Absorption processes occur on the cemented carbide surface, whose reflectivity plays an important role in the laser's efficiency. The energy absorption of cemented carbide surfaces varies from 76 to 77% at a wavelength of 1064 nm and it is 85% at a wavelength of 355 nm [10]. This absorption promotes a localized increase in temperature, which may cause ablation, i.e., a controlled explosion of liquid and gas phases due to the rapid heating. Considering the cemented carbide substrate, under low laser intensity the carbide phases remain almost untouched, with only the top peaks being melted. Cobalt vaporizes due to its high vapor pressure and, therefore, the overall effect is quite similar to abrasive sandblasting. Under high intensities, cemented carbide melts, presenting numerous scattered surface holes with an average size of 3–5 μm through which underlied gases are released [11]. The removal of material occurs mainly through ablation; hence, the thermal properties of carbide and cobalt play an important role [10].

When a cemented carbide surface is irradiated with a pulsed laser beam, thermal stresses occur during the heating and cooling cycles due to the rapid expansion and contraction of the irradiated region. Depending on the properties of the cemented carbide and the energy and duration of the laser pulse, levels of stress far exceeding the elastic limit can be generated, which may result in plastic deformation and cracking in the laser irradiated region. This is particularly true of carbides due to their high melting point and low thermal conductivity, which promote high temperature gradients. High residual stresses occur due to the difference between the thermal conductivities of carbide and cobalt, which may cause cracking in the carbide phase. The flow of melted cobalt toward the free surface may also favor its increased concentration close to the surface [12].

Uhlmann et al. [13] showed that laser texturing of cemented carbide (wavelength $\lambda = 355$ nm, focal diameter of 15 μm, pulse duration of 10 ps, pulsing frequency of 500 kHz, energy per pulse of 1 μJ, at a speed of 1 m/s) increases its surface roughness and the concentration of cobalt at the surface, irrespective of the initial condition of the surface. Laser ablation increases the adhesion between coating and substrate such that, in scratch tests, failure occurs in either the coating or the substrate. Laser treatment had shown to be more efficient than abrasive flow machining (AFM) to improve coating adhesion.

A variation of the texturing process carried out in air is the texturing of a target surface submerged in liquids. Its purpose is to use part of the light energy to vaporize water and form confined plasma. When the plasma collapses it produces a shock wave in the liquid and in the solid. Shock waves thus generated in the liquid adjacent to the surface carry particles away, causing a very efficient cleaning. Water also cools the surface more effectively than air, reducing the overall heating even more [14].

Arroyo et al. [15] performed milling tests to compare laser-treated against commercial tools. Their results indicated that there was no difference between the average tool life of the laser-textured and commercial MT-CVD tools. The wear profile of the laser-treated and commercial tools showed no remarkable differences. No significant differences in wear were found between the experimental laser pretreated and commercial sandblasted tools. Both laser treated and sandblasted tools presented similar tool wear mechanisms, which included diffusion, attrition, abrasion and chipping.

Table 1
Properties of the laser pulse incident on the cemented carbide.

Condition	A	B
Average power (W)	9.0	15.0
Peak power (kW)	6.9	11.5
Pulse energy (mJ)	0.9	1.5

On the other hand, milling tool life tests on compacted graphite iron showed the superior performance of laser textured PVD coated tools. The increased tool life of laser pre-textured tools coated with TiAlN and AlCrN can be attributed to the stronger mechanical anchoring of the coatings on the substrate. Modification of the substrate by laser radiation ensures a standardized texture, while microblasting creates a texture with disordered orientation, which does not ensure uniform mechanical anchoring of the coating [16].

In terms of using laser texturing on the substrate surface of cemented carbide tools, one point must still be addressed: What are the correct laser parameters to get the best coating–substrate adhesion and, consequently, the longest tool life? Just few works touched this point. The purpose of this work was to evaluate the effectiveness of laser texturing using different laser power, with the targeted sample under water and in the air, aiming to improve the adhesion between the coating layer and substrate of PVD coated tools and, consequently, improve tool life.

2. Materials and experimental procedures

The surfaces were textured using a frequency-doubled diode-pumped Nd:YAG laser system comprising a power source, a laser head and a computer to control the system. The laser wavelength was 532 nm (green), the pulsing frequency was 10 kHz, the pulse length was 130 ns, the spot diameter was 0.2 mm and the maximum power was 15 W at the workpiece. A set of prisms and lenses that directed the beam to a scanning system ensures the position of the pulses on the target surface. To control texturing of the entire surface, the distance between the centers of two neighboring pulses was 0.07 mm. The surface was textured three times and a 60° incremental rotation was applied between texturing runs.

Samples of TNMG 160408 QM1005 ISO grade P15 cemented carbide inserts (the tool supplier identifies this carbide grade as 1005) were gotten from the manufacturing process prior to the cleaning operation preceding the PVD process. This cemented carbide grade was composed only of WC and Co. Before texturing, the inserts were analyzed by scanning electron microscopy (SEM) and X-ray diffraction (XRD). After texturing the inserts returned to the regular manufacturing process for coating application. Fifty energy dispersive spectroscopy (EDS) analyses were performed along a line in each textured insert to identify changes in cobalt concentration. Eight inserts were laser textured under the conditions A or B as described in Table 1. These tools were, then, PVD coated with a TiAlN layer.

After the coating process, the inserts were analyzed again by SEM and XRD, followed by an evaluation of the coating adhesion by standard Rockwell C indentation tests. Indentations were made at three points on each insert clearance face, two adjacent to the tip (close to the cutting region) and one in the central region distant from the cutting region. Since the inserts had three clearance faces, each insert was indented nine times. The indentations were analyzed in a stereomicroscope linked to a computer through a camera under 50× magnification.

Dry cylindrical turning experiments were performed to evaluate and compare the life and wear of the laser textured and PVD coated inserts with those of commercial tools, hereinafter called standard tools, which had the same substrate, coating and geometry. These experiments were carried out on a CNC lathe with 15 kW

Table 2
Laser texturing and machining conditions.

Texturing		Turning parameters		
Average laser power (W)	Environment	v_c (m/min)	f (mm/rev)	a_p (mm)
9	Air	300 360		
	Water	300 360		
15	Air	300 360	0.1	0.5
	Water	300 360		
Standard		300 360	0.1	0.5

of power in the spindle motor and maximum spindle rotation of 4500 rpm. Table 2 lists the experimental parameters. Some of the laser-texturing processes were performed with the sample target submerged in a 4 mm thick layer of water, as also shown in Table 2.

The turning workpieces were cylindrical SAE 1045 steel bars with normalized dimensions of 100 mm diameter per 250 mm length, which were fixed on the lathe chuck and tailstock, leaving an unobstructed length of 230 mm available for cutting. Each turning experiment was concluded when the tool reached a flank wear of $V_B = 0.3$ mm. This point was considered the end of tool life. All the experiments were performed in triplicate. Tool wear was measured several times during the experiment using a stereomicroscope.

3. Results and discussion

The SEM analyses of as received cemented carbide substrate revealed a homogeneous grain structure, with an average grain size of 0.6 μm and a few grains of ∼3 μm (less than 1%). The average concentration of Co elements in the substrate surface was 5.8%. Successive EDS analyses along a line revealed the absence of surfaces with cobalt segregation before treatment, i.e., the cobalt concentration was homogeneous along the insert surface.

The photomicrographs in Fig. 1 illustrate the effect of laser texturing on two surfaces; one textured at 9 W and the other at 15 W both in air. The image of the surface textured at 9 W (Fig. 1(a)) indicates that the incident energy was insufficient to promote complete melting of all the surface carbide grains, since some partially melted grains remained in several regions. The grain boundaries in the melted region (right upper corner of Fig. 1(a)) were completely melted, without the presence of solidification cracks. The EDS analysis of the substrate textured at 9 W did not show any cobalt-rich regions; the cobalt content of this substrate was less than 5%.

Fig. 1(b) (surface textured at 15 W) shows complete melting of all the surface carbides. The entire sample shows the presence of pores formed by the released gases. Some pores are connected by small cracks, but they are not visible throughout the whole sample. Similarly to 9 W condition, the EDS analysis along a line on the surface textured at 15 W also found no cobalt-rich regions, even when the analysis was made close to the pores. Therefore, laser texturing caused a slight decrease in the surface Co content, which was, on average, 5.8% before texturing.

After coated, all the surfaces showed numerous defects (Fig. 2(a) and (b)), like the droplets adhered to the coating surface in Fig. 2 originated from the PVD coating process. Their average size was 3 μm, which is larger than the average grain size of the substrate. These droplets increase the roughness of the coating film and may work as crack initiation points, contributing to the adhesion of chips on the tool [17].

A higher magnification close to the substrate–coating interface (Fig. 2(c)) revealed a coating defect that hampers an accurate

measurement of its thickness. The average of 10 measurements indicated that the coating thickness was 1.8 ± 0.2 μm, which is about three times the average grain size of the substrate.

Fig. 3 clearly shows the difference between the textured and standard surfaces when the effect of texturing on adhesion was evaluated by the indentation method. No delaminating areas or cracks at the edges of the indented regions were visible on the textured surface, regardless the power (9 and 15 W) and the environment (air or water). Samples textured in water showed some micro-detachments close to the indentation marks, but the coating remained adhered to the surface. On the other hand, the standard inserts showed a large area of coating detached around the indentation. One explanation for this enhanced adhesion of the textured tools compared with the standard ones is the mechanical anchoring of the coating provided by the texturing process.

Textured surfaces presented higher surface roughness than standard substrates. The average roughness (R_a) was 0.43 and 0.62 μm for conditions 9 W and 15 W, respectively, compared to 0.26 μm for the standard substrate. This leads to the assumption that the textured substrate surface acts as a barrier against slipping of the coating layer, thus increasing the coating–substrate adhesion. Moreover, a rougher surface provides a larger area of contact with the coating, because the layer material might penetrate into the roughness valleys.

Fig. 4 shows three X-ray diffractograms of the tool before coating. Fig. 4(1) represents the standard substrate cleaned by sandblasting. All the peaks seen to be related to the WC carbide, without noticeable Co peaks, revealing a Co-free surface. Fig. 4(2) and (3) shows the substrates submitted to 9 and 15 W laser power, respectively. The peaks (a), (b) and (c), identify the WC_{1-x} phase formed as a consequence of partial decarburizing during laser treatment. The differences between 9 W and 15 W conditions are connected to the intensity of the peaks, because decarburizing increases with increasing temperature for the same processing time. Laser-induced chemical reactions allowed the migration of carbon atoms out of WC grain, forming the non-stoichiometric WC_{1-x}.

Fig. 5(1) shows the diffractogram of a standard tool before and after coating. Coated samples present two extra peaks identified (a) and (b) in Fig. 5(1). These peaks belong to the TiN (osbornite) phase.

Fig. 5(2) shows the laser-textured cemented carbide (15 W) before and after coating. Before coating, black curve in Fig. 5(2), extra peaks belonging to the WC_{1-x} appear approximately at the same position of the TiAlN peaks. Indeed the first four diffraction peaks of the non-stoichiometric carbide WC_{1-x} (36.98, 42.89, 62.03 and 74.20°) [22] are very near to the diffraction angles of the TiAlN coating (36.70, 42.63, 61.89 and 74.13°) shown by the red line in Fig. 5(1).
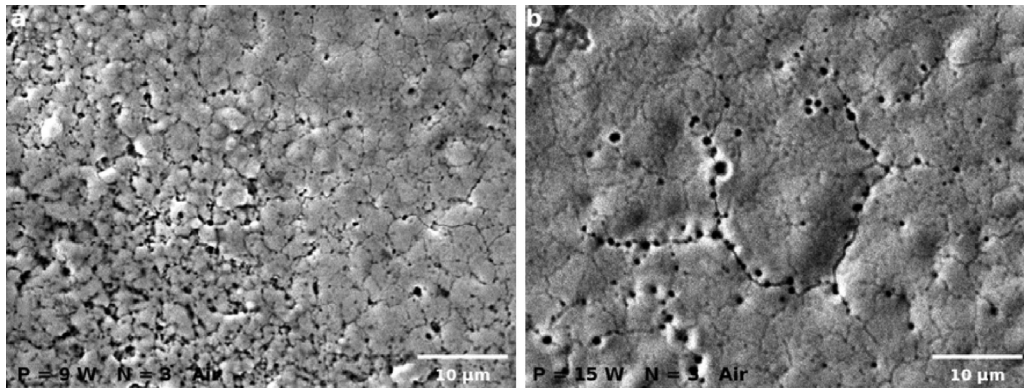
Fig. 1. Effect of laser radiation on the substrate microstructure: (a) surface textured in air with $P = 9$ W and (b) surface textured in air with $P = 15$ W.
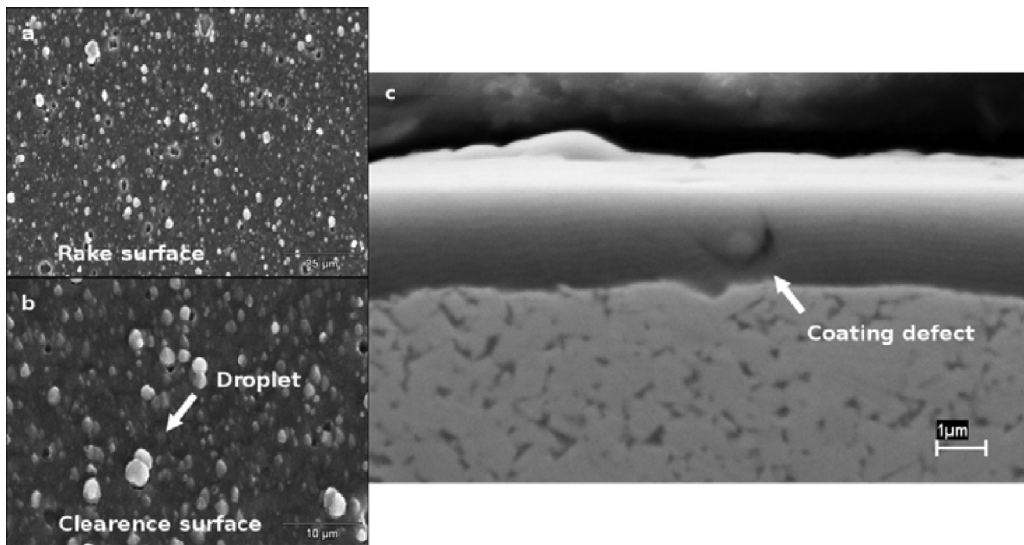

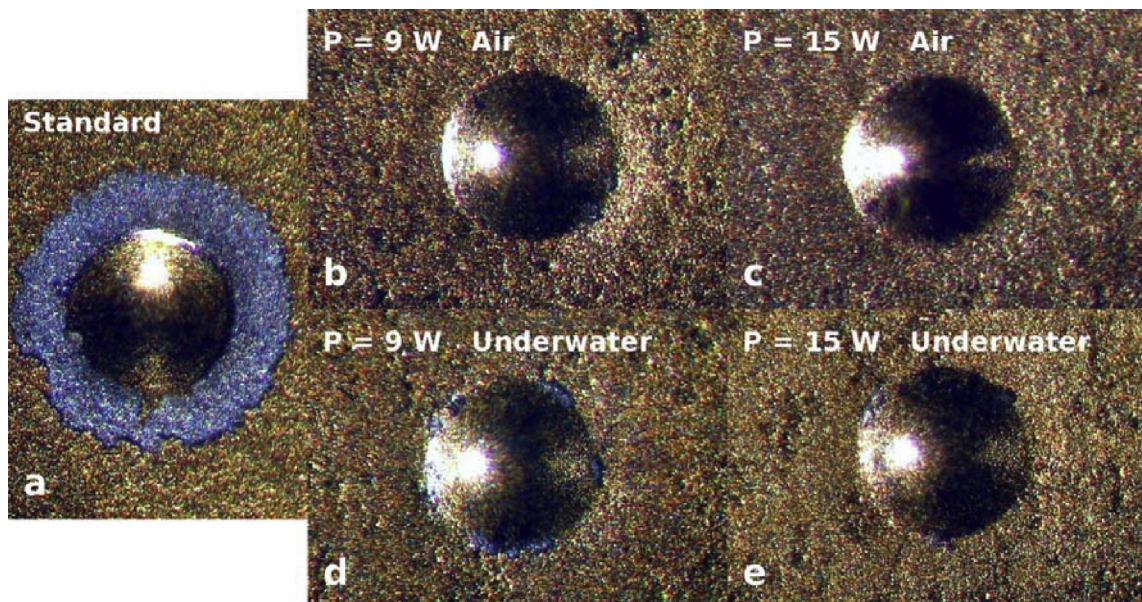**Fig. 2.** Defects of the coated inserts: (a) rake face; (b) clearance face and (c) substrate–coating interface.

Fig. 3. Indentation marks on the textured and standard surfaces.
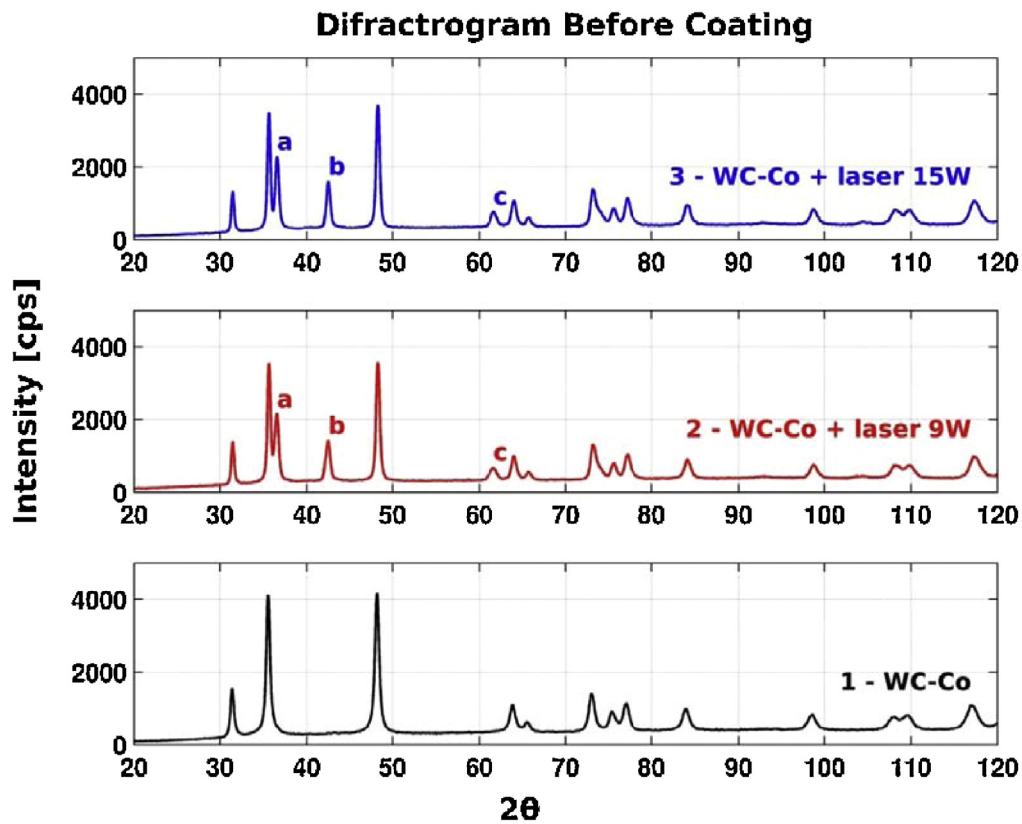
Difractrogram Before Coating

Fig. 4. Diffractogram of cemented carbide before coating: (1) sandblasted cemented carbide, (2) 9 W laser textured cemented carbide and (3) 15 W laser textured cemented carbide.

Both materials belong to the same Fm−3m(225) space group with a cubic crystal system with crystal lattice parameters *a*, *b* and *c* of 4.2355 Å for the WC_{1-x} and 4.2390 Å for the TiAlN. Therefore, laser texturing produces a chemical modification in the carbide exposed grains leading to a new phase with lattice parameters similar to the TiAlN phase.

Besides mechanical anchoring mechanisms caused by the higher surface roughness already cited, other possible explanations for the good adhesion of the coating on the substrate promoted by the laser process can be built. Firstly, the laser action cleans the surface, removing all its contaminants. Secondly, the localized heating causes ablation and chemical reactions on the surface, which decarburize the surface of the grains. The short time duration of the laser pulse (100 ns) keeps the reactions on the surface layer of the carbide grains. The new phase WC_{1-x} nucleates epitaxially from the WC grains and presents a crystal structure with lattice parameters very similar to the coating parameters (difference of 0.08%). Thirdly, the TiAlN phase grows from a very similar crystal structure offering conditions for enhanced chemical bonding between coating and substrate. This explanation agrees with Hultman and Sundgren [18] which states: "For PVD coatings grown at low temperatures, the adhesion can also be improved by using substrates
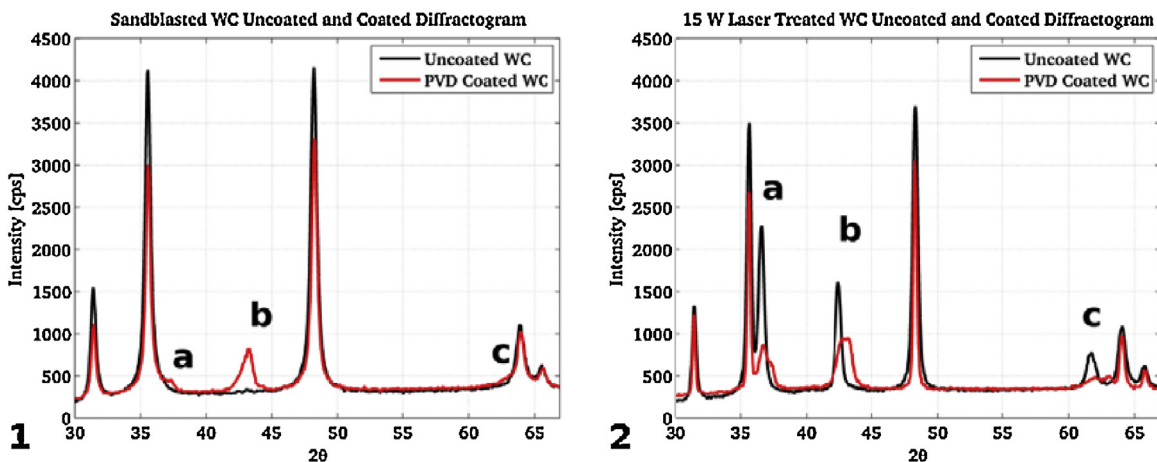

Fig. 5. Diffractograms of the standard (1) and laser textured with 15 W and (2) tools before and after coating.
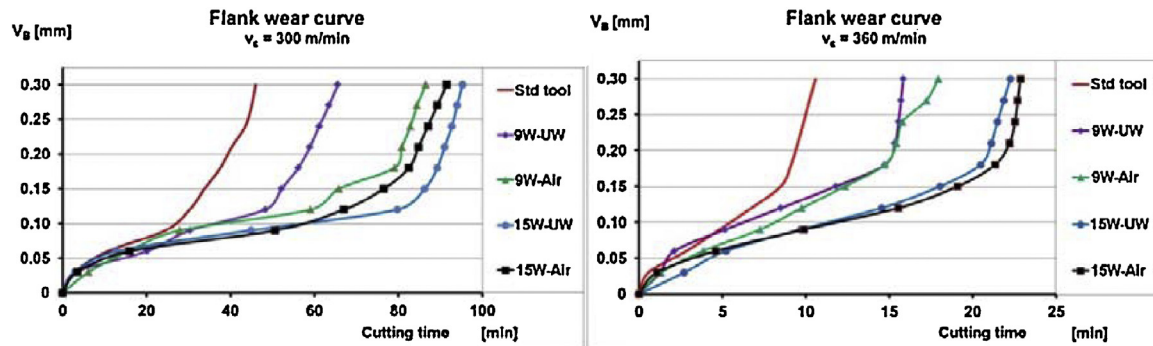
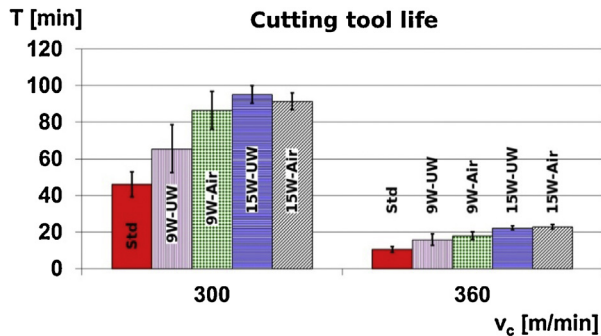**Fig. 6.** Tool flank wear curves of all the turning experiments.

Fig. 7. Tool lives of all the turning experiments.

that are structurally similar to the coating materials. A structural and chemical matching between coating and substrate results in a low interface energy, and thus, promotes high adhesion".

Fig. 6 shows the tool flank wear curves obtained using cutting speeds of 300 and 360 mm/min in the turning experiments. Each curve represents an average of the results obtained in three experiments performed in each speed condition. This figure clearly illustrates the longer lives of the textured tools compared to the conventional tools. At this point, it should be noted that all the flank wear curves (Fig. 6) presented the same behavior. After a short transient, the curves reached a constant slope that is approximately the same disregarding surface preparation, using laser or not. Then, depending on the cutting time, the slope suddenly increases as a result of wearing of the cutting edge. It is reasonable to assume that the point at which the slopes changed indicates where the coating had been removed and the substrate start to have contact with the chip and workpiece, thereby accelerating tool wear. Therefore, these curves indicate that the textured surfaces were able to hold the coating for longer periods, thus extending tool life.

Fig. 7 illustrates the tool lives obtained in all experiments. Each bar represents the average tool life for the three replications, while the error bars represent the dispersion of the replication results.

The results in Fig. 7 indicate that the higher coating–substrate adhesion of the textured tools presented in Fig. 3 resulted in longer tool lives than those obtained with standard tools. The tool life obtained with the tools textured at 15 W was on average double that of the standard tools. As can be seen in this figure, the texturing performed with a power of 15 W produced tools whose service life was longer than that of tools textured at 9 W. However, underwater texturing did not result in the increase of the tool lives, since it did not improve the adhesion between coating and substrate, as already was perceived in Rockwell C tests (Fig. 3). Additionally, it could be verified that a 20% increase in cutting speed (from 300 to 360 m/min) caused an average 75% reduction of tool life.

When texturing is done in water, refraction takes place. The difference between the refraction indexes of air and water changes the laser beam path before reaching the sample.

The beam waist increased in the case of water covered samples because of the defocusing. The defocusing is due to different refraction indexes of water and air, and thus decreased the intensity and fluence on the sample surface. This fact attenuates the severity of the laser interaction with carbide, causing smaller roughness on the carbide surface. The WC_{1-x} phase fraction generated is very low in under water-texturing when compared with the air condition. Since the $WC–WC_{1-x}$ formation is driven by laser heating, and water environment provided much more heat transfer than normal air, the occurrence of WC_{1-x} phase was decreased in underwater experiments.

The Rockwell C tests proved to be consistent with the machining test for qualifying the better processing parameters. The only result that was not completely consistent was that obtained with the tools textured at different laser powers. The indentation results showed no difference between the tools textured at 9 and 15 W, and the life of tools textured at 15 W was longer than that of tools textured at 9 W. The reason for this discrepancy may be that the static load imposed on the tools by indentation tests did not suffice to highlight the difference in adhesion between these two textured tools. Only dynamic tests like the machining tests were able to impose a sufficiently high load on the tools to reveal the difference in adhesion between the tools textured at 9 W and at 15 W. However, it should be kept in mind that texturing at 15 W generated rougher surfaces than texturing at 9 W, which enabled stronger mechanical anchoring of the coating to the substrate and thus resulted in longer tool life. It is possible to suppose that an even rougher surface finish would eventually produce better results than those obtained at 15 W. However, the experimental apparatus is limited to this power level. Ohring [19] reported that an increase of surface roughness in the region where a sudden change in material occurs (from the substrate to the coating material) contributes to increase mechanical anchoring, thus contributing to better adhesion between coating and substrate. Tönshoff et al. [2] also stated that the larger contact area resulting from increased surface roughness improves the adhesion of PVD coating to the substrate. On the other hand, the mechanical attachment efficiency of the coating–substrate system must reach a maximum, given by the current mechanical conditions during cutting operation.

Fig. 8 shows the flank wear is one of the standard tools used in the turning experiments performed at a cutting speed $v_c = 300$ m/min. The purpose of analyzing these SEM micrographs is to identify the wear mechanisms that caused the end of life of the cutting edge. These photomicrographs were therefore taken at the end of tool life. In this figure, it could be noted that the main defects was caused by notch wear. Note, also, that flank wear occurred (region 3 in Fig. 8(a)) between the notches (regions 1 and
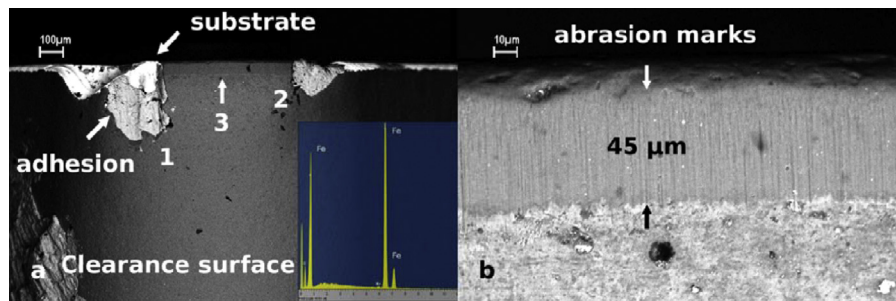
Fig. 8. Flank wear land of the standard tool. $v_c = 300$ m/min, $f = 0.1$ mm/rev. (a) View of the flank wear land and (b) magnification of region 3.

2 in Fig. 8(a)), but it was much smaller than the notches. Therefore, notch wear increased at a much faster rate and was responsible for the end of tool life.

Pavel et al. [20] asserted that the mechanical action of the chip edge, oxidation and chemical interaction between chip and tool are the mechanisms that generate notch wear. Notch wear caused the removal of the tool coating and was triggered by the attrition mechanism. Attrition wear can be described as the cyclic adhesion and removal of workpiece/chip material from the tool, which also causes removal of tool particles. Under these conditions, microscopic particles of the tool are pulled out and dragged away together with the material flow [21]. The occurrence of attrition is indicated by the abundant presence of chip/workpiece material (Fe) in the notch region. This was detected in the EDS analysis of points 1 and 2 also depicted in Fig. 8(a).

Unlike regions 1 and 2, whose coating film was completely removed (Fig. 8(a)), the central region of the wear land (region 3 – Fig. 8(a)) showed intact coating film (without exposure of the substrate). A magnified image of this region (Fig. 8(b)) reveals a surface with abrasive marks (scratches parallel to the cutting direction). This region was devoid of droplets (see Fig. 2(a) and (b)), indicating that the abrasion mechanism was responsible for their removal. These droplets, together with the particles removed by abrasion, acted as a third body in the abrasion process. The height of the abrasive scratches was 45 μm at the moment of the end of tool life. This finding indicates that the abrasion process, that very likely was stronger in the region of notch wear (board of the chip–tool contact) due to the harder chip edge, caused the coating removal in this region and, consequently, opened the way for the attrition mechanism, what, as already said, triggered the notch wear. This finding also indicates that, in the other experiments in which flank wear (not notch wear) was responsible for the end of tool life, and the attrition mechanism was responsible for the increase in flank wear (as will be discussed in greater detail later), the initial wear mechanism was abrasion. Therefore, the coating film was removed by the abrasion mechanism, creating the necessary conditions for the adhesion of chip/workpiece material on the wear land, which is indispensable for the attrition mechanism to occur.

Fig. 9 shows the flank wear land of a textured tool (9 W of laser power in air) processed at a cutting speed of 300 m/min. At the beginning of the turning tests, the textured tools presented minor notch wear with an average height of no more than 150 μm, which is smaller than the tool life criterion ($V_B = 0.3$ mm). Regardless of the laser texturing condition, this wear mechanism was the first to appear and was detected by stereomicroscopic observation during the tests. As the experiment continued, other flank wear mechanisms became predominant and the notch wear stabilized, unlike what occurred with the standard tools. Therefore, it can be concluded that the higher substrate–coating adhesion enabled by the texturing process succeeded on halting the progression of notch wear. One of the causes of notch wear is the mechanical action of the

chip edges against the tool [21]. Therefore, due to the high adhesion promoted by the texturing process, the chip edges were too weak to remove a large quantity of tool particles, thereby preventing the progression of notch wear.

A large adhesion of chip/workpiece material is visible in the flank wear land in Fig. 9(a) (in this image, note the strong presence of Fe detected by EDS). Detail 1, which is magnified in Fig. 9(b), shows the minor notch wear present in this wear land. Visible between the notch and the region with adherent material are abrasion marks with heights of about 55 μm (see Fig. 9(b)), which was not sufficient to expose the substrate.

After reaching a value of no more than 0.15 mm, the notch wear stabilized and the region of adhesion depicted in Fig. 9(a) became predominant in the flank wear land. The removal of the coating film which enabled the adhesion of the chip/workpiece material on the flank face, and hence, the occurrence of the attrition phenomenon, was very likely caused by the abrasive process, as indicated by the abrasive scratches illustrated in Fig. 9(b). After the coating was removed from the flank face by abrasion, the adhesion of workpiece material prevailed in the formation of flank wear, as indicated in Fig. 9(a).

Adherent material is cyclically renewed during the cutting process. Rubbing against the workpiece removes this material from the flank face, the workpiece flow carries it away and a new portion of chip/workpiece material adheres to the wear land. However, the connection between adhered material and tool is not broken at their interface. Frequently, this break occurs in the tool material and hard tool particles are removed through the workpiece flow, rubbing against the workpiece and tool and acting as a third body in the abrasion mechanism. This phenomenon is a second source of wear in the attrition mechanism (the first is the removal of tool particles through the removal of chip/workpiece material), which further aggravates tool wear [21]. Since the tool life obtained with the tools textured with a laser power of 15 W was longer than that obtained with the tools textured at 9 W, and since the wear mechanisms on the tool textured at 15 W were very similar to those on the tool textured at 9 W, it can be assumed that the higher coating adhesion obtained with higher laser power delayed, but did not change, the wear mechanisms. Additionally, when the coating started to wear, a more fine and regular pieces of the coating were detached in the 15 W condition, thus causing less tool damage.

A comparison of the wear mechanisms of the standard and textured tools indicated that they presented the same wear mechanisms. All the mechanisms acting upon the standard tools were also active in the textured tools. However, because the texturing increased the adhesion between the coating film and the substrate (see Fig. 3), it changed the significance of the wear mechanisms. All the tools showed notch wear, which was responsible for the end of tool life of the standard tools and also shortened their service life. The formation of notch wear was accelerated by the lack of adhesion between the coating film and the tool substrate. In the textured
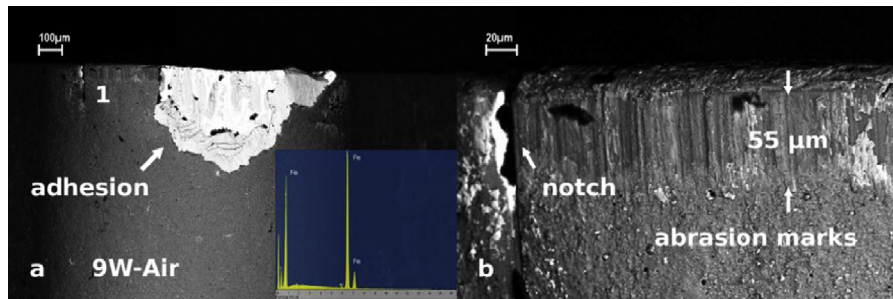
Fig. 9. Flank wear land of a textured tool (9 W of laser power in air). v_c = 300 m/min, f = 0.1 mm/rev. (a) View of the flank wear land and (b) magnification of region 1.

tools, the notch formed at the beginning of tool life stabilized after reaching small heights (much smaller than the tool life criterion). The progression of this wear was inhibited by the strong adhesion that texturing promoted between coating and substrate, which prevented the coating from becoming detached at the cutting edge. One of the main factors that trigger the notch wear mechanism is abrasion of the tool by the chip edges, which are very hard due to the hardening they undergo in response to the strong deformation to which they are subjected. The higher coating–substrate adhesion of the textured tools hindered the removal of coating fragments, causing the chip edges to rub against a very hard surface, i.e., the coating. Therefore, the mechanism of notch formation in textured tools was much slower than in standard tools. Once the notch formation was hindered, attrition assumed a more important role in the formation of wear, and was the mechanism responsible for the end of tool life of textured tools.

Although the hypothesis of mechanical anchoring of the coating to the substrate due to the higher surface roughness of laser textured surfaces has been cited repeatedly in this paper and in the literature as the cause for the greater adhesion of the coating to the substrate of laser textured tools, other effects may be also considered.

One important aspect of the partial decarburizing during laser treatment is that the WC_{1-x} and TiAlN phases present almost the same crystal structure (cubic crystal structure, class Fm−3m-225) and similar lattice parameter. Since the decarburizing of cemented carbide occurred in a tiny layer next to the grains exposed to the laser radiation, it could be presumed that a composition gradient next to the upper surface of the carbide grains occurred. Also, as the coating crystal structure is very similar to the exposed grain structure (WC_{1-x}) the growth could occur epitaxially. If a pure epitaxial growth could be promoted here, the enhanced adhesion characteristics of the laser treated cemented carbide tools were due to two separated mechanisms: (a) mechanical anchoring due to the induced roughness and (b) chemical affinity between substrate and coating.

4. Conclusions

Based on the results of this work, and in conditions similar to those used here, it can be concluded that:

- Laser textured substrates presented increased roughness without inducing cobalt segregation toward the free surface.
- Substrate laser texturing induced the formation of WC_{1-x} carbides replacing the WC carbides of the original substrate.
- The WC_{1-x} phase produced at the grains surface by the laser treatment has crystal structure very similar to the TiAlN phase of the coating.
- The adhesion between the TiAlN PVD coating and the substrate (measured by the Rockwell C indentation method) of the laser textured tools was better than that of the standard tools.

- Laser texturing in air produced slightly better coating–substrate adhesion than texturing in water.
- The flank wear curves indicated that the laser textured tools kept their coating longer in the turning experiments, thus increasing the tool life.
- The laser textured tools had longer tool lives than the standard ones. The tools textured in air with the higher laser power showed the longest tool life.
- The kind of wear responsible for ending the tool life was notch wear in the standard tools and flank wear in the laser textured tools.
- The mechanism that produced notch wear (likely the abrasion between the hardened chip edges and the tool) was hindered by the stronger adhesion between coating and substrate of the laser-textured tools. This prolonged the tool life and caused the attrition wear phenomenon to be responsible for the formation of flank wear in laser textured tools.

References

[1] M. Ali, E. Hamzah, N. Ali, Adhesion strength of tin coatings at various ion etching deposited on tool steels using cathodic arc PVD technique, Surface Review and Letters 16 (2009) 29–35.
[2] H.K. Tönshoff, C. Blawit, K.T. Rie, A. Gebauer, Effects of surface properties on coating adhesion and wear behaviour of PACVD-coated cermets in interrupted cutting, Surface and Coatings Technology 97 (1997) 224–231.
[3] H.K. Tönshoff, A. Mohlfeld, C. Gey, J. Winkler, Surface modification of cemented carbide cutting tools for improved adhesion of diamond coatings, Surface and Coatings Technology 108–109 (1998) 543–550.
[4] H.K. Tönshoff, A. Mohlfeld, Surface-treatment of cutting-tool substrates, International Journal of Machine Tools and Manufacture 38 (1998) 469–476.
[5] K.-D. Bouzakis, N. Michailidis, S. Hadjiyiannis, K. Efstathiou, E. Pavlidou, G. Erkens, S. Rambadt, I. Wirth, Improvement of PVD coated inserts cutting performance, through appropriate mechanical treatments of substrate and coating surface, Surface and Coatings Technology 146–147 (2001) 443–450.
[6] S. Creasey, D.B. Lewis, I.J. Smith, W.-D. Münz, SEM image analysis of droplet formation during metal ion etching by a steered arc discharge, Surface and Coatings Technology 97 (1997) 163–175.
[7] J. Gerth, U. Wiklund, The influence of metallic interlayers on the adhesion of PVD TiN coatings on high-speed steel, Wear 264 (2008) 885–892.
[8] M. Verdier, S. Costil, C. Coddet, R. Oltra, O. Perret, On the topographic and energetic surface modifications induced by laser treatment of metallic substrates before plasma spraying, Applied Surface Science 205 (2003) 3–21.
[9] V.V. Semak, N.B. Dahotre, in: B. Narendra, Dahotre (Eds.), Lasers in Surface Engineering, ASM International, Materials Park, OH, 1998, pp. 35–67.
[10] G. Dumitru, B. Lüscher, M. Krack, S. Bruneau, J. Hermann, Y. Gerbig, Laser processing of hardmetals: physical basics and applications, International Journal of Refractory Metals and Hard Materials 23 (2005) 278–286.
[11] T. Li, Q. Lou, J. Dong, Y. Wei, J. Liu, Modified surface morphology in surface ablation of cobalt-cemented tungsten carbide with pulsed UV laser radiation, Applied Surface Science 172 (2001) 331–344.
[12] B.S. Yilbas, A.F.M. Arif, C. Karatas, M. Ahsan, Cemented carbide tool: laser processing and thermal stress analysis, Applied Surface Science 253 (2007) 5544–5552.
[13] E. Uhlmann, S. Richarz, V. Mihotovic, Substrate pre-treatment of cemented carbides using abrasive flow machining and laser beam ablation, Production Engineering 3 (2009) 81–86.
[14] A. Kruusing, Underwater and water-assisted laser processing: Part 1—General features, steam cleaning and shock processing, Optics and Lasers in Engineering 41 (2004) 307–327.

[15] J.M. Arroyo, A.E. Diniz, M.S.F. Lima, Wear performance of laser precoating treated cemented carbide milling tools, Wear 268 (2010) 1329–1336.

[16] M.P. Suarez, E.M. Martins, M.S.F. Lima, F.J. Silva, A.R. Machado, Laser textured coated tools used in turning process, 9 pp., in: Proceedings of COBEM 2011, 21st Brazilian Congress of Mechanical Engineering, ABCM, October 24–28, 2011, Natal, RN, Brazil, CD1, 2011.

[17] J. Gerth, M. Larsson, U. Wiklund, F. Riddar, S. Hogmark, On the wear of PVD-coated HSS hobs in dry gear cutting, Wear 266 (2009) 444–452.

[18] L. Hultman, J.E. Sundgren, in: R.F. Bunshah (Ed.), Handbook of Hard Coatings, William Andrew Publishing, New York, 2001, pp. 108–180.

[19] M. Ohring, The Materials Science of Thin Films, first ed., Academic Press, San Diego, 1991.

[20] R. Pavel, I. Marinescu, M. Deis, J. Pillar, Effect of tool wear on surface finish for a case of continuous and interrupted hard turning, Journal of Materials Processing Technology 170 (2005) 341–349.

[21] P.K. Wright, E.M. Trent, Metal Cutting, fourth ed., Butterworth-Heinemann, Boston, 2000.

[22] ICDD, International Centre for Diffraction Data, Powder Diffraction File ICDD-PDF: 20-1316, 2002.